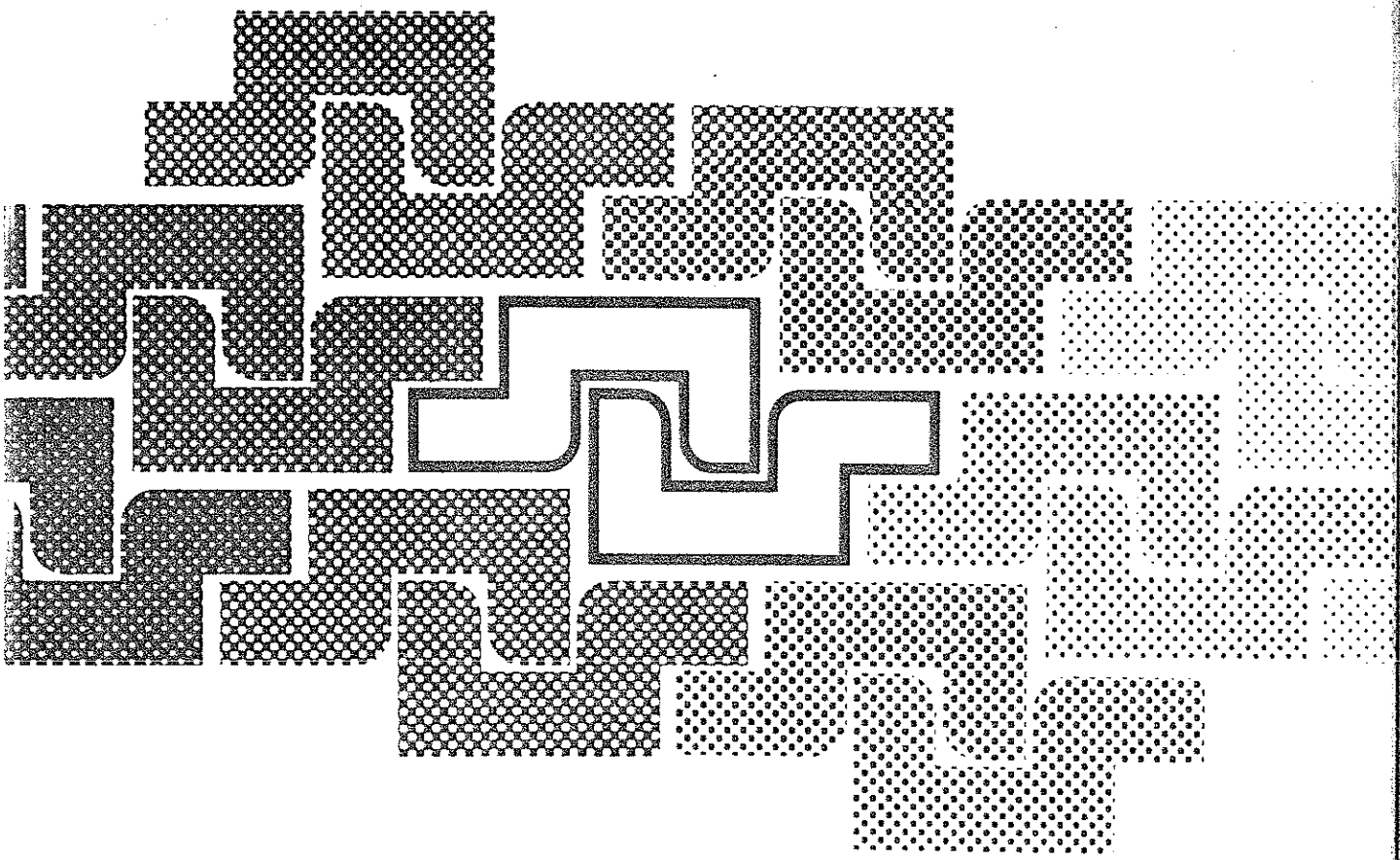

Vortex Flows and Related Numerical Methods

Edited by

J.T. Beale, G.-H. Cottet and S. Huberson

NATO ASI Series

Series C: Mathematical and Physical Sciences - Vol. 395

Vortex Flows and Related Numerical Methods

edited by

J.T. Beale
Department of Mathematics,
Duke University,
Durham, North Carolina, U.S.A.

G.-H. Cottet
Laboratoire de Modélisation et Calcul,
Université Joseph Fourier,
Grenoble, France

and

S. Huberson
Université du Havre,
Le Havre, France

Kluwer Academic Publishers

Dordrecht / Boston / London

Published in cooperation with NATO Scientific Affairs Division

NUMERICAL STUDY OF THE MOTION AND DEFORMATION OF TWO-DIMENSIONAL BUBBLES BY A VORTEX METHOD

HENRYK KUDELA
Technical University of Wrocław
50-370 Wrocław
Wybrzeże Wyspiańskigo 27
Poland

ABSTRACT. In this paper are presented numerical results that relate to the motion and deformation of a thermal bubble in a gravity field. The study was done using the vortex blob method. To regularize the initial value problem for the vortex sheet a parameter δ^2 was introduced in the Biot-Savart formula. We point out the viscous character of the δ^2 regularization. The evolution of circular and elliptical bubbles was studied. The numerical experiments showed great sensitivity of the evolved forms to the initial conditions.

1. Introduction

In the field of fluid mechanics it is well-known that a density difference between two fluids causes motion of the fluids. One of the most important problems within the general area of pattern formation and bubble mechanics relates to interface deformations. In this paper our interest concerns the evolution of the two-dimensional bubble in a gravity field when the fluid inside the bubble is slightly less dense than in an ambient fluid. Gravity causes the lighter fluid to accelerate in the direction of the heavier one. The interface of the bubble undergoes the classical Rayleigh-Taylor instability [Sharp, 1984]. The evolution of the bubble progresses to conditions "far from an equilibrium". One can expect that the future shape of the bubble will be very sensitive to the initial condition and will undergo unexpected changes. When the final shape of the bubble does not resemble its initial one, we may speak about morphological instability [Langer, 1980] [Sekerka, 1973]. If we make some simplifying assumptions about the physics (see below), the interface between the bubble and surrounding fluid can be regarded as a vortex sheet. The motion study of the bubble can be reduced to an initial value problem. Throughout the paper, we will assume that density variations are small. This allows us to significantly simplify the evolution equations for the vortex sheet and enables us to avoid some problems related to nonlinearity of these equations (Kudela 1990a,b). Instead of the Fredholm integral equation of the second kind, a simple differential equation has to be solved. This case still has practical interest, .e.g. in the study of the motion of a thermal [Scorer, 1978]. For the solution of the initial value problem we use the

J.T. Beale et al. (eds.), Vortex Flows and Related Numerical Methods, 191–205.

generalized vortex method described by Baker, Merion, Orszag (1980, 1982). It is known that the initial value problem for a vortex sheet is ill-posed in the Hadamard sense [Moore, 1979] [Krasny, 1986a]. At a finite time, the solution has a singularity. This is a consequence of the fact that the linear approximation yields an arbitrarily large growth rate for short-wavelength perturbations. From the practical point of view, the emergence of a singularity is physically unacceptable and shows inadequacy of the mathematical model in describing the problem. So it is reasonable to include certain physical mechanisms like diffusion, interfacial tension or the finite thickness of the interfacial transition region to regularize the problem. Another way to regularize the problem is to slightly change the original equations, as was done by Krasny [Krasny, 1986b] for the Kelvin-Helmholtz instability problem. He introduced into the formulas which describe the velocity induced by the vortex sheet (the Biot-Savart formula) a δ^2 parameter in such a way that the singular integrand is replaced by a smooth one [Krasny, 1986b]. This kind of regularization, by analogy to the Chorin vortex blob method [Chorin & Bernard 1973] is called vortex blob regularization. Krasny showed [Krasny, 1986b] that the δ^2-linearized equations give a bounded rate of growth for short wavelength perturbations. For the Rayleigh-Taylor problem it was shown [Bellman & Pennington, 1954] that viscosity causes the linear growth rate to vanish asymptotically with wavelength, and the same occurs for the δ^2 equations. So, although the introduction of δ^2 is a quite formal procedure and does not correspond precisely to any physical effect, one can interpret the introduction of the δ^2 parameter as a trial to mimic fluid viscosity.

2. Statement of the problem and equations of motion

We assume that the motion of the fluids is potential, two-dimensional, inviscid, and incompressible, and that the pressure across the interface is continuous (no surface tension effects). A rectangular system of coordinates (x,y) is introduced. The constant acceleration of gravity g acts in the negative y-direction. The densities of the fluids are constant and change their value across the interface. The density ρ_1 of the ambient fluid is slightly greater than the density ρ_2 of the fluid inside the bubble. The basic control parameter of the problem is the Atwood number:

$$A = \frac{\rho_1 - \rho_2}{\rho_1 + \rho_2} \tag{1}$$

The interface is described parametrically as $(x(e,t),y(e,t))$, where t is time and e is a real parameter $\in [0,1]$ which is used also as a Lagrangian variable. At the initial instant, the value of e marks a point which follows the motion of the interface. The initial shape of the bubble is described by an ellipse $(x(e,0),y(e,0)) = (a\cos(2\pi e), b\sin(2\pi e))$, where a and b are the large and small semiaxes of the ellipse. Moreover the ellipse can be rotated by an angle θ, where θ is the angle between the large axis of the ellipse and the horizontal x-axis. So the initial position and shape of the bubble can be characterized by the angle θ and the ratio $\beta = b/a$. Except for the case of a circle ($\beta = 1$), we present results only for the evolution of the ellipse with $\beta = 1/3$, $a = 1$ and for a different angles θ. The interface can

be regarded as a vortex sheet with strength equal to the tangential velocity jump across the interface:

$$\Gamma(s,t) = (\mathbf{u}_2 - \mathbf{u}_1)\,\mathbf{s}^{\circ} \tag{2}$$

where $\mathbf{u}_1, \mathbf{u}_2$ are the limiting velocities of the fluids at the interface, $\mathbf{s}^o$ = unit tangential vector, s = arclength. Due to the assumption that $\rho_1 \cong \rho_2$ we apply the Boussinesq approximation $A \mapsto 0$, $g \mapsto \infty$, such that Ag remains finite, $Ag = 1$. Equations describing the evolution of the bubble interface are:

$$\frac{\partial x}{\partial t} = -\frac{1}{2\pi}\int_0^1 \frac{\gamma(e',t)(y(e,t) - y(e',t))}{r^2 + \delta^2} d\,e' \tag{3}$$

$$\frac{\partial y}{\partial t} = \frac{1}{2\pi}\int_0^1 \frac{\gamma(e',t)(x(e,t) - x(e',t))}{r^2 + \delta^2} d\,e' \tag{4}$$

$$\frac{\partial \gamma}{\partial t} = 2\frac{\partial y}{\partial e} \tag{5}$$

where $r^2 = (x(e,t) - x(e',t))^2 + (y(\epsilon,t) - y(e',t))^2)^2$, and $\gamma(e,t) = \Gamma(e,t)(x_e^2 + y_e^2)^{1/2}$. Equations (3), (4) describe the velocity induced by the vortex sheet (Biot-Savart law, where we have already introduced δ^2), and equation (5), in the Boussinesq approximation, describes the vortex sheet strength. The units used in (3), (4) are such that length is scaled by the length of the large semiaxis of the ellipse a and time is scaled by $(a/Ag)^{1/2}$. For the rest of the paper we assume $a = 1$.

3. The numerical approximation

The vortex sheet was divided into N segments and the curve $(x(e,t), y(e,t))$ was approximated by $(x_i, y_i) = (x(e_i,t), y(e_i,t))$, $e_i = ih$, $h = 1/N$. The integrals in (3) and (4) were approximated by the trapezoidal rule at the alternate points [Shelley, 1992]. This yields a system of ordinary differential equations for the trajectories of the points and their strengths as follows:

$$\frac{dx_i}{dt} = -\frac{h}{\pi} \sum_{\substack{k=1 \\ k+i=odd}}^{N} \frac{\gamma_k(y_i - y_k)}{r_{ik}^2 + \delta^2} \tag{6}$$

$$\frac{d\,y_i}{dt} = \frac{h}{\pi} \sum_{\substack{k=1 \\ k+i=odd}}^{N} \frac{\gamma_k(x_i - x_k)}{r_{ik}^2 + \delta^2} \tag{7}$$

$$\frac{d\,\gamma_i}{dt} = 2\frac{d\,y_i}{d\,e} \tag{8}$$

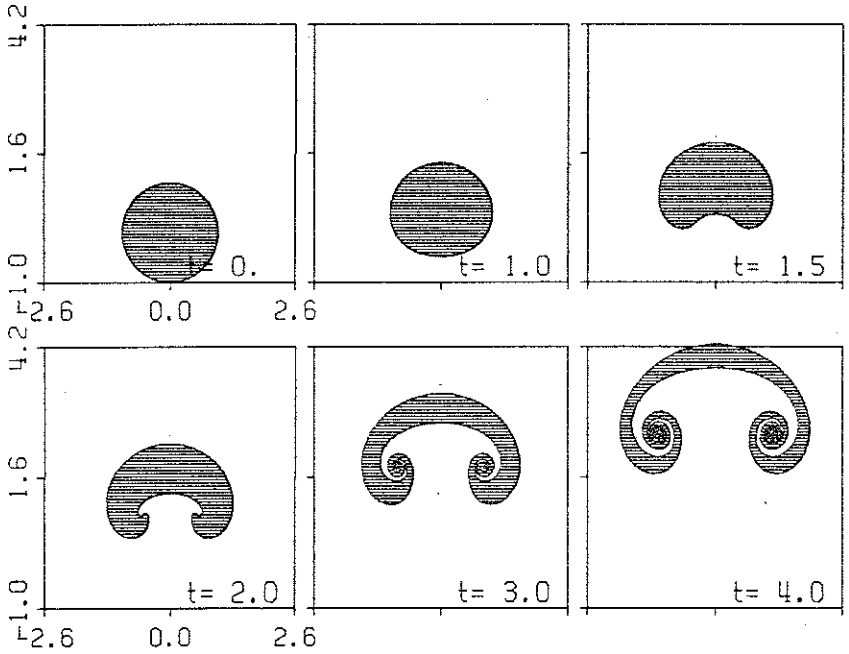

Fig. 1. Successive stages in the evolution of the circular bubble with $\delta^2 = 0.01$, $N = 600$. The time is indicated in the lower right corner of each frame.

The numerical procedure goes as follows [BMO, 1982]: for known $x(e)$, $y(e)$, $\gamma(e)$ the interface is marched forward using (6) and (7); next $\gamma(e)$ is also marched in time by using (8). The time stepping is performed by using the fourth-order Adam-Multon predictor-corrector scheme. To start calculations a Runge-Kutta (RKF45) algorithm was used. The derivative dy/de was calculated by a cubic spline. To check the accuracy, two invariants of the motion were monitored: the mass S of the bubble (it should be constant) and the mass flux Ω through the interface (it should be zero):

$$S = \int_0^1 y x_e de\,, \qquad \Omega = \int_0^1 \mathbf{u}\cdot\mathbf{n} de \tag{9}$$

When the relative error for S reached the value 0.025, or Ω reached .05, the calculation was stopped.

4. Numerical results

4.1. MOTION OF THE CIRCULAR BUBBLE

A numerical study of this case by the vortex method has already been done by Meng & Thomson (1978) and Anderson (1985) (but by another vortex method). We repeated those calculations in order to gain some understanding of the δ^2 influence. In Fig. 1 successive stages are shown in the evolution of the circular bubble for $\delta^2 = 0.01$. The spiral structure on both sides of the vertical axis of symmetry is clearly visible. In Fig.2 a close-up frame for $t = 4.$ from Fig.1 is presented.

A smaller value of δ^2 causes greater flexibility of the vortex sheet for roll-up. As δ^2 approaches to zero, the number of the turns in the spiral structure grows (see

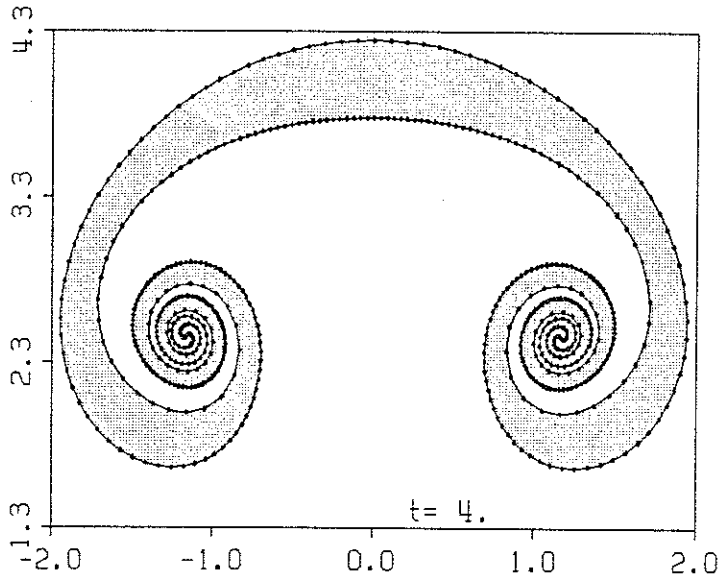

Fig. 2. Close-up of the frame for $t = 4$ from fig.1 . The points on the interface indicate the position of the markers moving with Lagrangian velocity ($N = 600$).

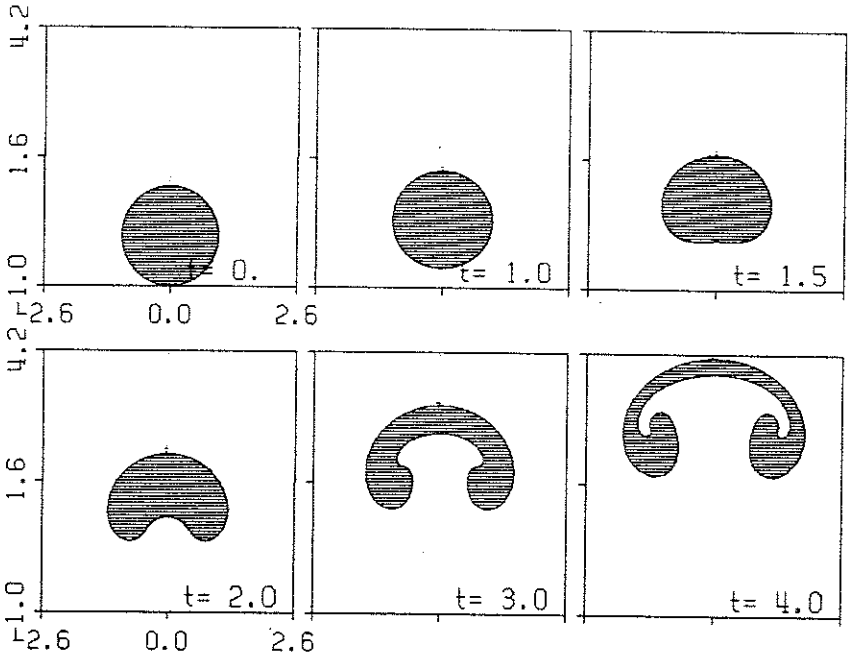

Fig. 3. Successive stages in the evolution of the circular bubble with $\delta^2 = 0.1$.

also [Krasny, 1986b], [Anderson, 1985]). A large value of δ^2 prevents any vortex sheet roll-up at all. In Fig.3 the evolution of the bubble for $\delta^2 = 0.1$ is shown. To illustrate the influence of the value of δ^2, solutions are shown in Fig. 4 which were obtained for a different δ^2 ($= 0.1$, $= 0.04$, $= 0.01$) at the same time $t = 4$.

One can see that while large scales of the bubble suffer only slight changes, the spiral structure becomes more and more complicated when the value of δ^2 is decreased. Intuitively a greater value of δ^2 corresponds to the effect of greater viscosity of the fluid. In Fig.5 we present the velocity of the upper point of the

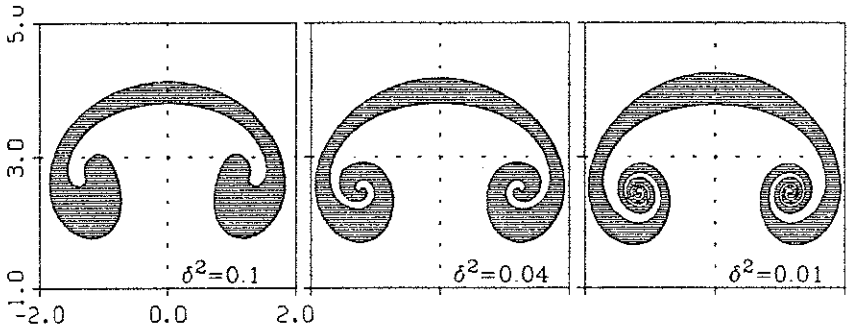

Fig. 4. Effect of δ^2. Interface at $t = 4.$ with δ^2 value as shown.

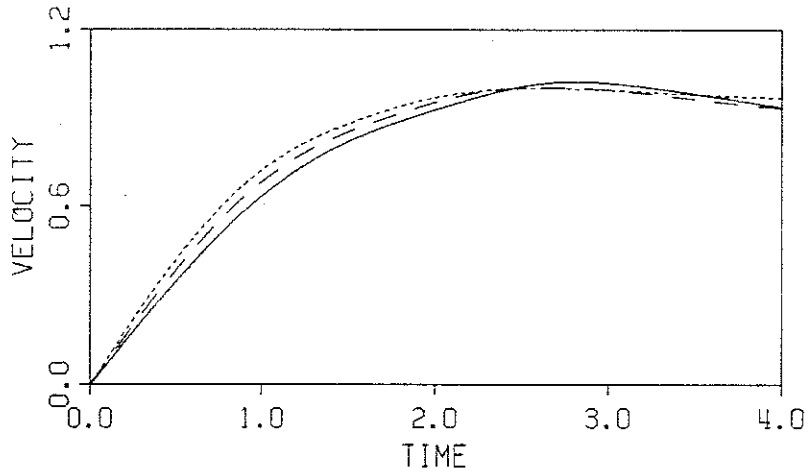

Fig. 5. Velocity of the upper point of the bubble vs. time. — $\delta^2 = 0.1$, − − − $\delta^2 = 0.04$, $\cdots$ $\delta^2 = 0.01$.

bubble on the symmetry axis vs. time, and in Fig.6 the thickness of the cap vs. time for different values of the δ^2 parameter. The rate of change of the total vorticity in one half of the curve is measured by the thickness Δy of the cap on the symmetry axis; integration of (5) with respect to ϵ in interval $[0, 0.5]$ gives $\frac{\partial}{\partial t}\int_0^{0.5}\gamma = -2\Delta y$. Fig.5 suggests that a limit for the bubble velocity may exist independently from the δ^2 value. A greater value of δ^2 (more "viscous" fluid) causes a slower raising of velocity (Fig.5), and the total rate of change of vorticity drops ("dissipates") more quickly (Fig.6).

4.2. MOTION OF THE ELLIPTICAL BUBBLE

In actual experiments the initial shape of the bubble would most likely not be circular (of course it would never be two-dimensional as well). For this reason it was interesting to study the case of the evolution of a bubble that was not circular at the initial instant. We assumed that the initial form of the bubble would be an ellipse. Its shape was to be characterized by the ratio of the small axis of the ellipse to the large one $\beta = b/a$ and by the angle θ between the x-axis of the coordinate system and the large axis of the ellipse. In this paper numerical results are presented only

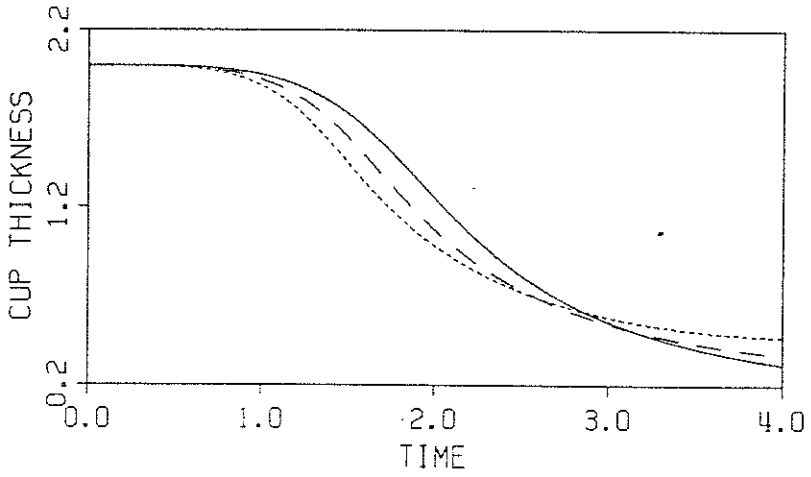

Fig. 6. Cap thickness vs time. — $\delta^2 = 0.1$, – – – $\delta^2 = 0.04$, $\cdots$ $\delta^2 = 0.01$.

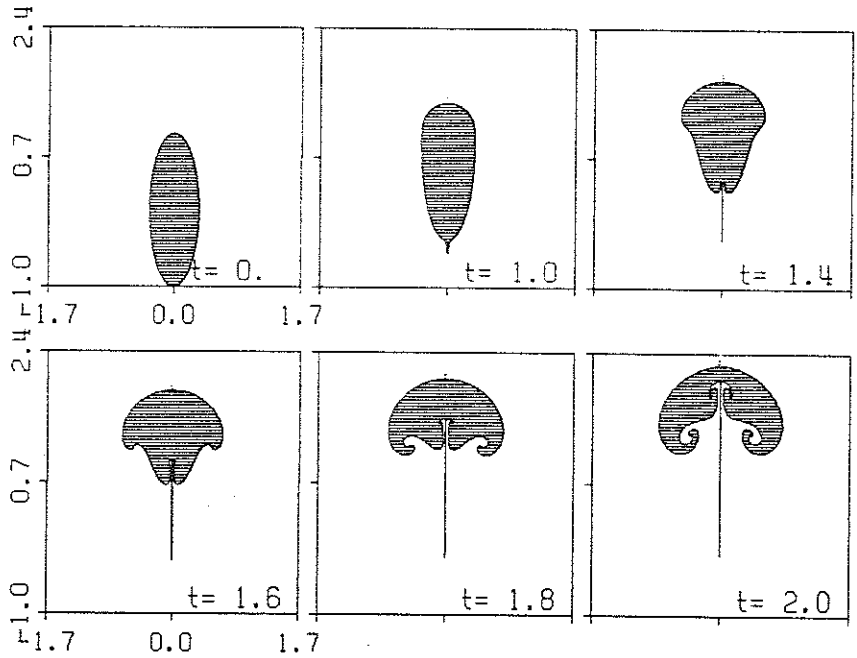

Fig. 7. Successive stages in the evolution of the elliptical bubble with $\theta = 90$, $\beta = 1/3$, $\delta^2 = 0.01$, $N = 600$.

for $\beta = 1/3$ but with different θ. In Fig.7 the successive stages are shown for the evolution of the bubble for $\beta = 1/3$, $\theta = 90^o$ and $\delta^2 = 0.01$. (See close-up portraits for $t = 1.8$ and $t = 2$ in Fig.8.)

At first one may be struck by the development of the tail structure. Such a tail was observed in many experiments [Kojima, Hinch & Acrivos, 1984] [Sparrow, Husar & Goldstein, 1970] [Griffithes, 1986]. The surrounding fluid penetrates the bubble near the base of the tail. The tail (fluid thread) is stretched, and its thickness at some point goes to zero; at this point probably the tail will be separated from the bubble (see[Kojima, Hinch & Acrivos, 1984]). Due to the relatively small value of δ^2, the back side of the bubble undergoes very fine deformation and undulation. The front of the bubble takes the shape of a circle. A greater value of δ^2 prevents

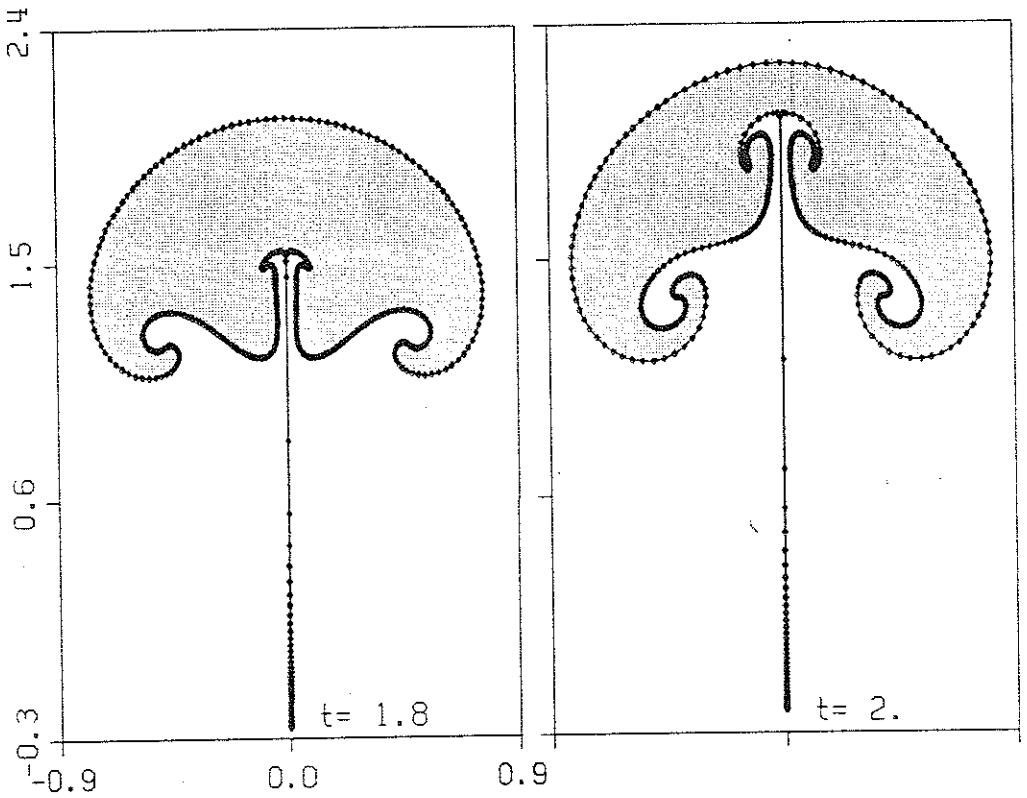

Fig. 8. Close-up of the two frames from Fig.7 for $t = 1.8$ and $t = 2$. ($\delta^2 = 0.01$, $\theta = 90^o$, $N = 600$)

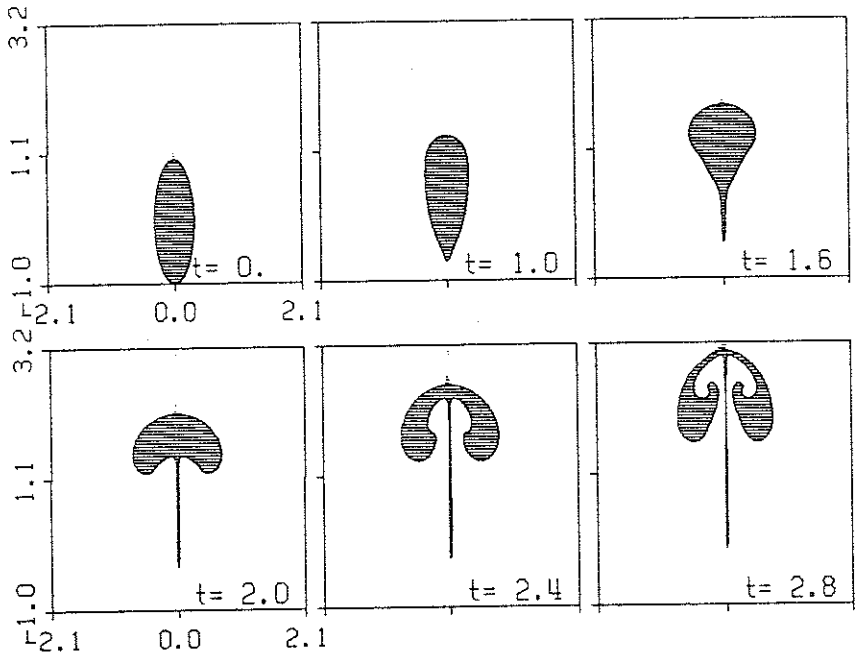

Fig. 9. Successive stages in the evolution of the elliptical bubble with $\theta = 90$, $\beta = 1/3$, $\delta^2 = 0.04$.

such fine undulating deformation of the interface. The tail becomes slightly thicker. Greater values of δ^2 change the time scale of deformation. Evolution progresses more slowly (see Fig.9).

In Fig.10 the evolution of the bubble is presented for $\theta = 60^o$ and $\delta^2 = 0.01$.

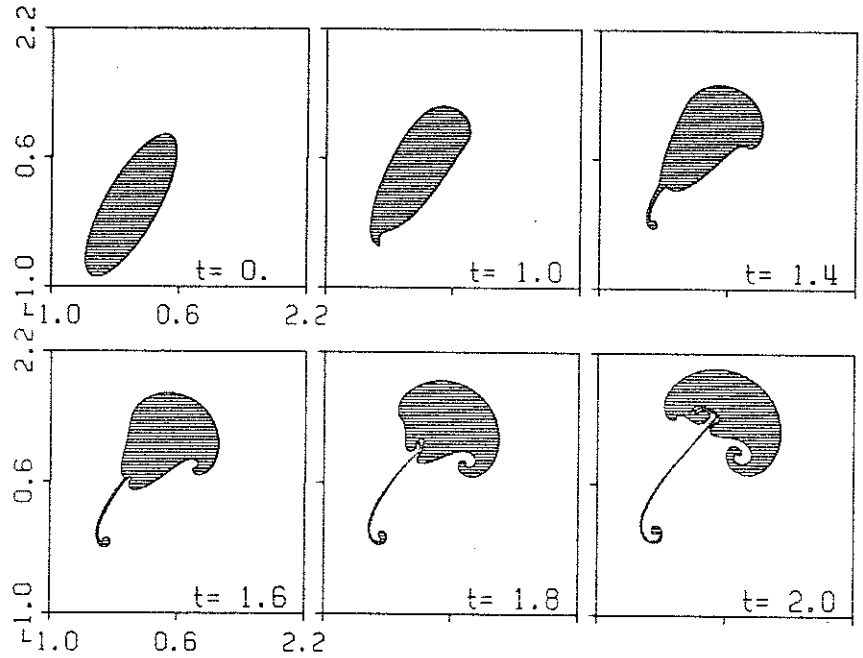

Fig. 10. Successive stages in the evolution of the elliptical bubble with $\theta = 60$, $\beta = 1/3$, $\delta^2 = 0.01$, $N = 800$

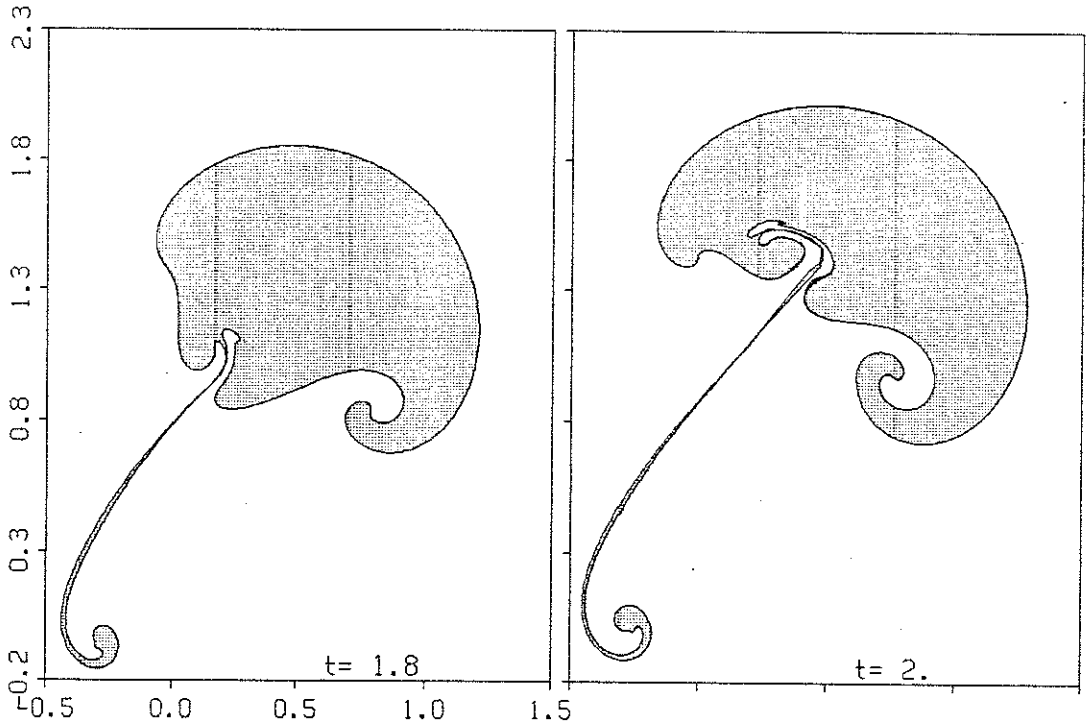

Fig. 11. Close-up of the two frames from Fig.10 for $t = 1.8$ and $t = 2.(\delta^2 = 0.01, \theta = 60^\circ, N = 800)$

Due to the relatively small δ^2 (compare with Fig.7) the rear side of the bubble was strongly undulated (see close-up portraits in Fig.11).

As previously, greater values of δ^2 makes the back side of the bubble smoother

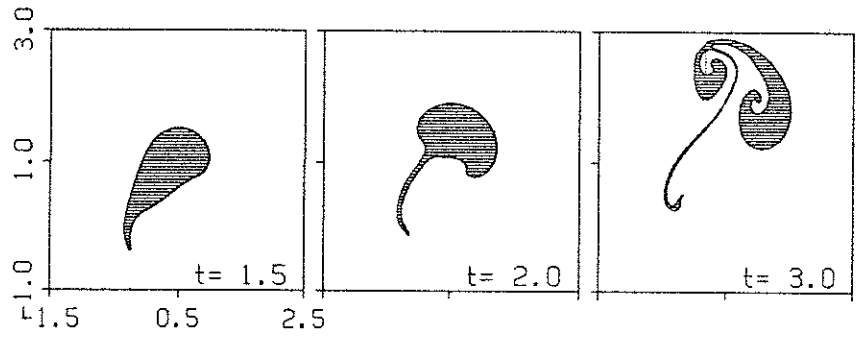

Fig. 12. Final stages of the elliptical bubble evolution with $\theta = 60$, $\beta = 1/3$, $\delta^2 = 0.04$.

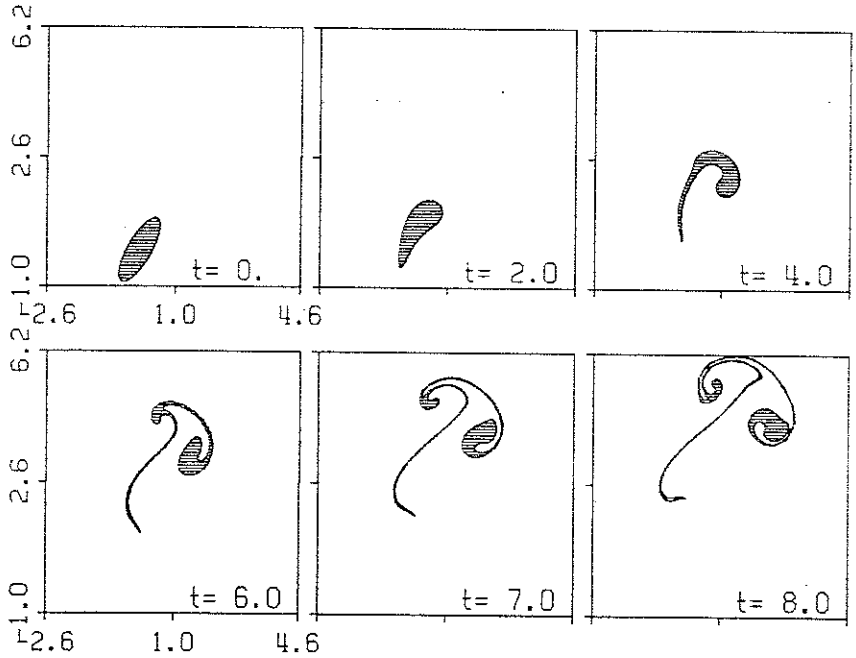

Fig. 13. The successive stages of the bubble in evolution for $\delta^2 = 0.4$, $\theta = 60°$, $N = 600$.

(Fig.12).

Greater values of δ^2 not only change the time scale of deformation and give a smoothing effect but may also considerably change the shape of the bubble during the evolution. In Fig. 13 we present the evolution of the bubble for $\theta = 60^o$ (as in Fig.10) but with $\delta^2 = 0.4$. Deformation of the bubble progresses very slowly and in the final stages the front of the bubble is composed of a thin thread (see close-up portraits for $t = 7$ and $t = 8$ in Fig.14).

In Fig.15 the evolution of the elliptical bubble for $\theta = 45^o$, and $\delta^2 = 0.04$ is presented.

In the following figures we present results for the bubble evolution for the same initial angle $\theta = 30^o$ and for different δ^2 values, $\delta^2 = 0.01$, .04, and 0.4. Once more we can notice the influence on the evolution of the initial angle θ (compare with Fig.10 and 15) and the modification caused by the different values of δ^2.

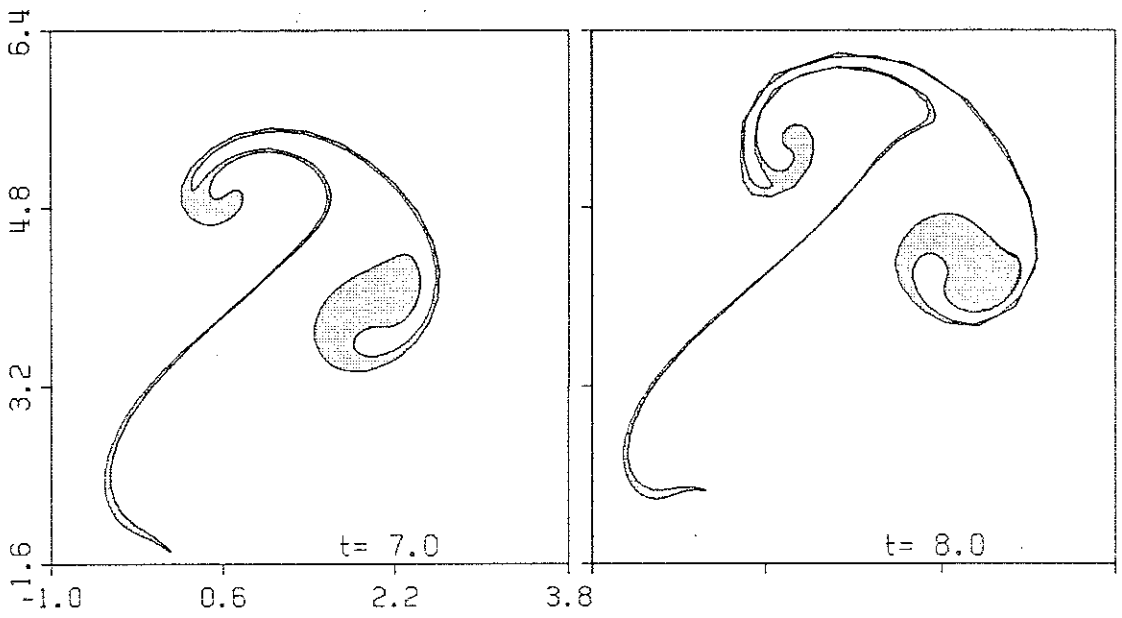

Fig. 14. Close-up portrait of the bubble from Fig.13 for $t = 7$ and $t = 8$. ($\delta^2 = 0.4$, $\theta = 60°$, $N = 600$)

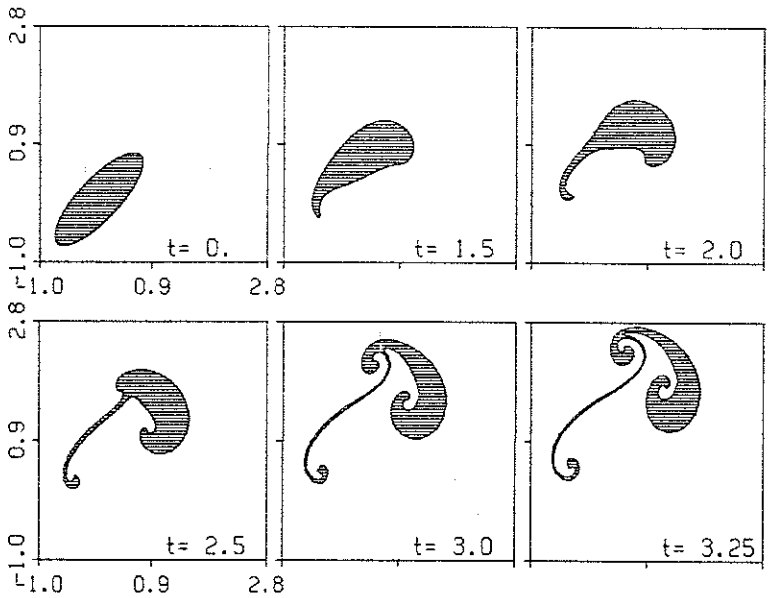

Fig. 15. The successive stages of the bubble in evolution for $\delta^2 = 0.04$, $\theta = 45°$, $N = 600$.

5. Concluding remarks

This work was inspired mainly by the work of Aref (1987) and Langer (1980) in the context of "dynamical morphology". We were interested in the evolution of the forms that progress in unstable conditions or as one has called it, "far from

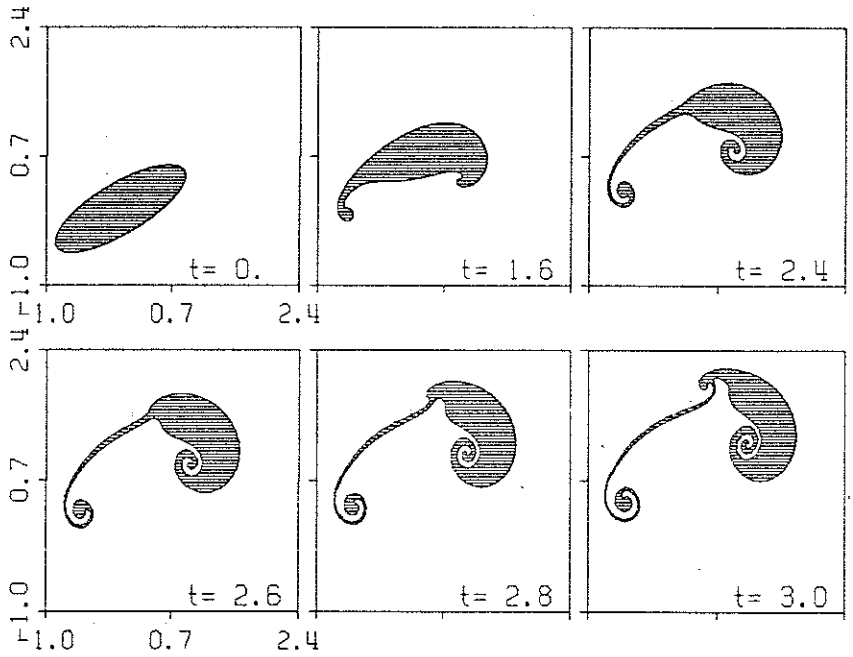

Fig. 16. The successive stages of the bubble in the evolution for $\delta^2 = 0.01$, $\theta = 30^o$, $N = 800$.

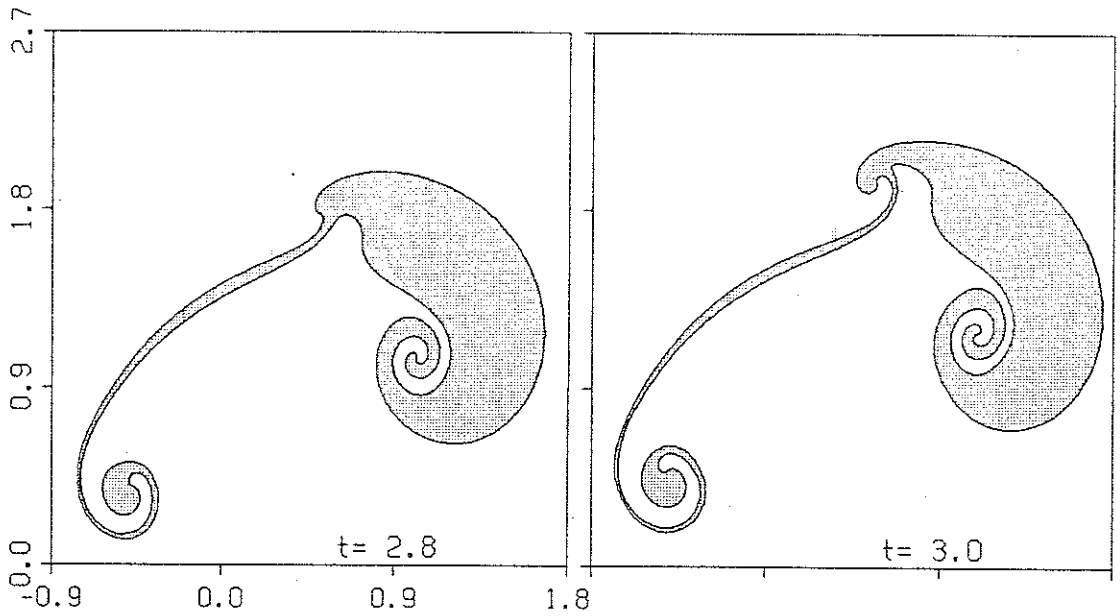

Fig. 17. Close-up of the two portraits from Fig.16 for $t = 2.8$ and $t = 3.0$ ($\delta^2 = 0.01$, $\theta = 30^o$, $N = 800$).

equilibrium". Evolution in such situations inevitably develops strange forms, where in its final stages such entities should emerge as "whorls, tendrils and spikes" [Aref, 1987]. Our results indicate that the tail structure appears due to initially non-circular (elliptical) shapes of the bubble. For the symmetrical case ($\beta = 1/3$, $\theta = 90^o$) our results agree qualitatively, despite the two-dimensionality of our model, with the experimental investigation of Kojima *et al.* (1984) (up to the moment when in the experiment the tail was cut off from the bubble) and the numerical one

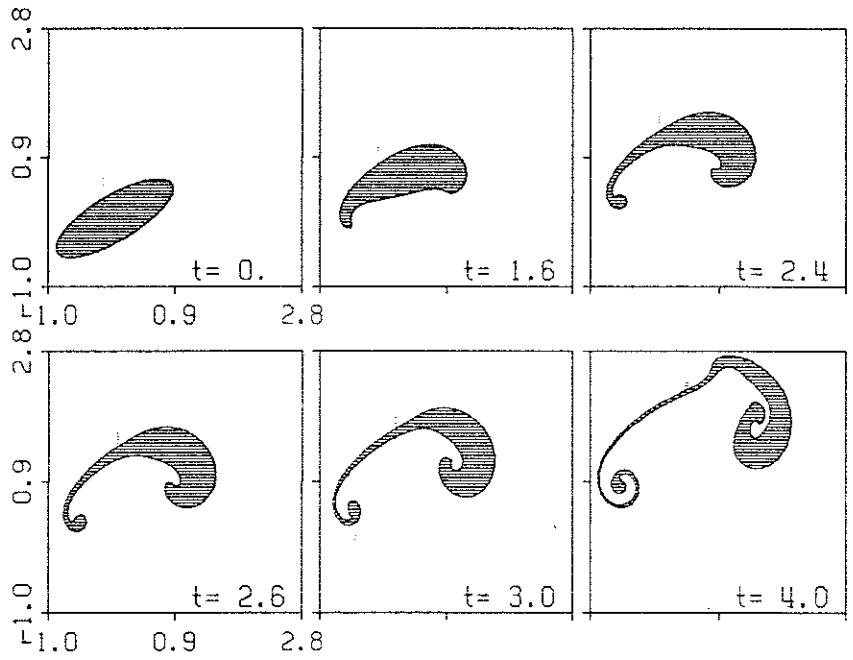

Fig. 18. The successive stages of the bubble in the evolution for $\delta^2 = 0.04$, $\theta = 30°$, $N = 600$.

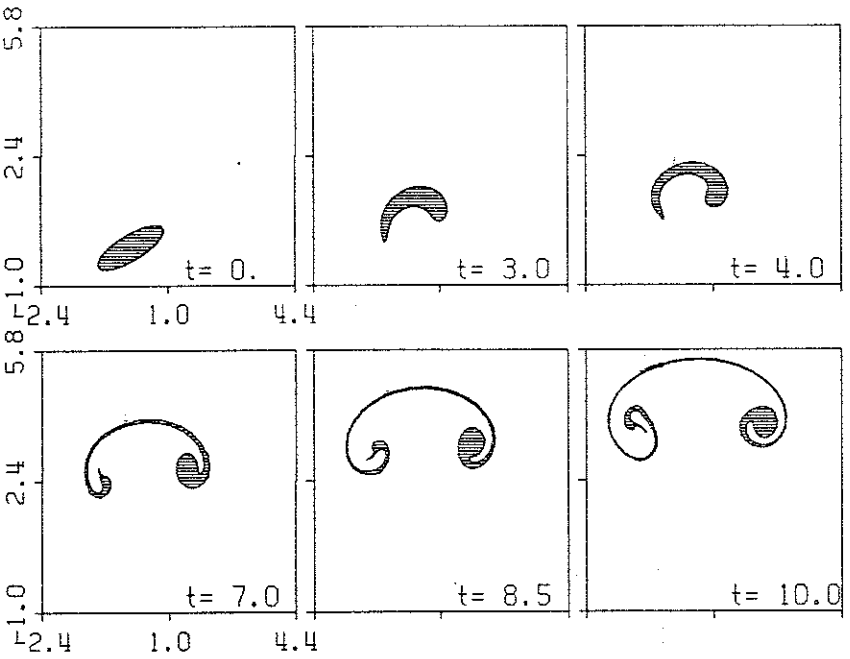

Fig. 19. The successive stages of the bubble in the evolution for $\delta^2 = 0.4$, ($\theta = 30°$, $N = 600$)

[Pozrikidis, 1990]. As we expected, the shape of the bubble during its evolution is sensitive to the initial condition (the angle θ). We did not refer to the problem of the existence of the limit solution when $\delta \mapsto 0$ (see [Krasny, 1986b]). Our feeling is that such a limit may not exist in the case of Rayleigh-Taylor instability but that some other indications like velocity may converge as $\delta \mapsto 0$. Blob regularization gives results which look more realistic than without it. The δ^2 value may strongly modify the bubble evolution. Due to the simplicity of the mathematical model

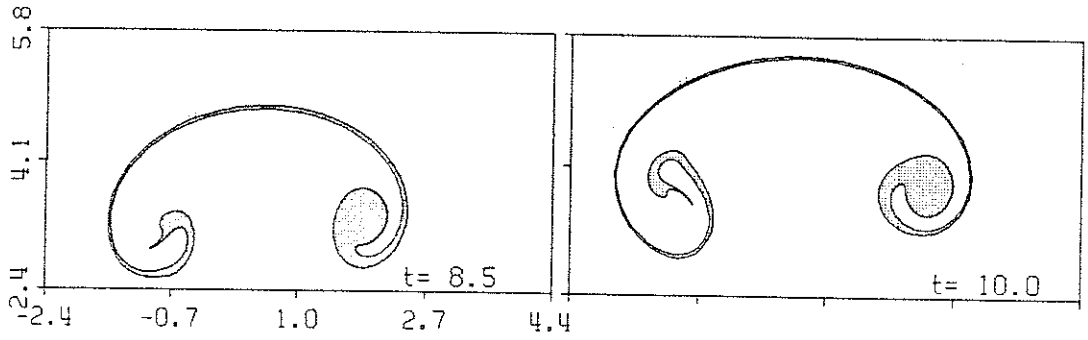

Fig. 20. Close-up of the two portraits from Fig.19 for $t = 8.5$ and $t = 10$. ($\delta^2 = 0.4$, $\theta = 30^\circ$)

and a not very involved numerical algorithm, the program is very convenient for investigation of diverse aspects of morphological instability.

Acknowledgements

The work was supported by Grant Nr 1542/3/91 from the Polish Committee of Scientific Investigation.

References

Anderson, 1985 Anderson C.R. 1985 *A vortex method for flows with slight density variations.* J. Comput. Phys. **61**, 417-444.

Aref, 1987 Aref H. 1987 *Finger, bubble, tendril, spike.* Fluid Dynamics Transactions, **13**, 25-54, Warszawa PWN.

BMO, 1980 Baker G.R., Merion D.I., Orszag S. A. 1980 *Vortex simulation of the Rayleigh-Taylor instability.* Phys. Fluids, **23**, 1485-1480

BMO, 1982 Baker G.R., Merion D.I., Orszag S.A. 1982 *Generalized vortex methods for free-surface flow problems.* J. Fluid Mech. **123**, 477-501.

Bellman & Pennington, 1954 Bellman R., Pennington R.H. 1954 *Effects of surface tension and viscosity on Taylor instability.* Quart. Appl. Math. **123**, 151-162.

Chorin & Bernard 1973 Chorin A.J., Bernard P.S. 1973 *Discretization of a vortex sheet with an example of roll-up.* J. Comput. Phys. **13**, 423-429.

Griffithes, 1986 Griffithes R.W. 1986 *Thermals in extremely viscous fluids, including the effects of temperature-dependent viscosity.* J. Fluid Mech. **166**, 115-138.

Kojima, Hinch & Acrivos, 1984 Kojima M., Hinch E.J., Acrivos A. 1984 *The formation and expansion of a toroidal drop moving in a viscous fluid.* Phys.Fluids **27**(1), 19-32.

Krasny, 1986a Krasny R. 1986 *A study of singularity formation in a vortex sheet by the point-vortex approximation.* J. Fluid Mech. **167**, 65-93.

Krasny, 1986b Krasny R. 1986 *Desingularization of periodic vortex sheet roll-up.* J. Comput. Phys. **65**, 292-313.

Kudela, 1990a Kudela H. 1990a *The influence of the surface-tension effects on using vortex method in the study of Rayleigh-Taylor instability.* Notes on Numerical Fluid Mechanics **29**, 273-282, ed. P.Wesseling, Vieweg.

Kudela, 1990b Kudela H. 1990b *Numerical studies of Rayleigh-Taylor instability by vortex method.* Arch. Mech. **42**, 493-505.

Kudela, 1992 Kudela H. 1992 *Study of the motion of the two-dimensional bubble by the vortex method.* Z. Angew. Math. Mech. **72**, 5, 369-373.

Langer, 1980 Langer J.S. 1980 *Instability and pattern formation in crystal growth.* Rev. Modern Physics **52**, 1-27.

Meiron, Baker & Orszag, 1982 Meiron D.I., Baker G.R., Orszag S.A. 1982 *Analytical structure of vortex sheet dynamics, Part 1. Kelvin-Helmholtz instability.* J. Fluid Mech. **114**, 283-298.

Meng & Thomson, 1978 Meng J. S., Thomson J.A.L. 1978 *Numerical studies of some nonlinear hydrodynamic problems by discrete vortex element method.* J. Fluid Mech. **84**, 433-453.

Moore, 1979 Moore D.W. 1979 *The spontaneous appearance of singularity in the shape of an evolving vortex sheet* Proc.R.Soc.Lond. A365, 1

Pozrikidis, 1990 Pozrikidis S.C. 1990 *The instability of a moving viscous drop.* J. Fluid Mech. **210**, 1-21.

Scorer, 1978 Scorer R.S. 1978 Environmental Aerodynamics. Halsted Press.

Sparrow, Husar & Goldstein, 1970 Sparrow E.M., Husar R.B, Goldstein R. J. 1970 *Observations and other characteristics of thermals.* J. Fluid Mech. **41**, 793-800.

Sharp, 1984 Sharp D.H. 1984 *An overview of Rayleigh-Taylor instability.* Physica **12D**, 3-18.

Shelley, 1992 Shelley M.J. 1992 *A study of singularity formation in vortex sheet motion by a spectrally accurate vortex method.* to be published in J. Fluid Mech.

Sekerka, 1973 Sekerka R.F. 1973 *Morphological stability.* in Crystal Growth: an Introduction, ed. P. Hartman.